Biophysical Journal Volume 97 November 2009 2577–2584

Large Structural Change in Isolated Synaptic Vesicles upon Loading with Neurotransmitter

Kristi L. Budzinski,[†] Richard W. Allen,[†] Bryant S. Fujimoto,[†] P. Kensel-Hammes,[‡] David M. Belnap,[§] Sandra M. Bajjalieh,[‡] and Daniel T. Chiu[†*]

[†]Department of Chemistry and [‡]Department of Pharmacology, University of Washington, Seattle, Washington; and [§]Department of Chemistry and Biochemistry, Brigham Young University, Provo, Utah

ABSTRACT The size of a synaptic vesicle (SV) is generally thought to be determined by the amount of lipid and membrane protein it contains. Once formed, it is thought to remain constant in size. Using fluorescence correlation spectroscopy and cryogenic electron microscopy, we show that glutamatergic vesicles reversibly increase their size upon filling with glutamate. The increase (~25% in diameter) corresponds to an increase in surface area of ~50% and in volume of ~100%. This large size increase implies a large structural change in the SV upon loading with neurotransmitters. Vesicles lacking SV protein 2A (SV2A) did not manifest a change in size after loading with glutamate, indicating that SV2A is required for this phenomenon.

INTRODUCTION

Synaptic vesicles (SVs) are small organelles (~40 nm in diameter) that mediate quantal chemical communication between neurons (1,2). SVs can be viewed as distinct compartments defined by a lipid bilayer, and their size is generally thought to be determined by the amount of membrane they contain. Neurotransmitters are loaded into SVs by transporter proteins in their membrane that utilize an electrochemical gradient to drive transmitter uptake. This gradient is established by a vacuolar-type ATPase that uses energy derived from ATP hydrolysis to translocate protons into the vesicle interior, thus creating both a pH gradient and a potential gradient that fuels the uptake and storage of the transmitter (2).

Previous studies using slices (3) and cultured PC12 cells (4) reported that vesicles with greater numbers of vesicular transporters (3) or neurotransmitters (4) have a larger average size in electron microscopy (EM) images. This size increase was assumed to be caused by incorporation of additional membrane proteins (e.g., transporters (3)) or lipids into the vesicle, because a membrane-dominated organelle would not be able to increase its size significantly without incorporating additional materials into the lipid bilayer. For example, synthetic lipid vesicles burst when their diameter is increased by a mere ~0.7% to ~2.5% (corresponding to a critical areal strain of 1.3–5.1%), depending on the composition of the membrane (5).

Here, we show that isolated SVs in solution reversibly increase in size after filling with the neurotransmitter glutamate, with no apparent addition of lipid or protein molecules. This suggests that SVs undergo large structural changes as the vesicle fills with neurotransmitter, and that the presence of the neurotransmitter may be encoded in the vesicle size.

MATERIALS AND METHODS

SV isolation

SVs were isolated from commercially purchased stripped rat brains (Pel-Freeze, Rogers, AR) or from green fluorescent protein (GFP)-transfected (synaptopHluorin) mouse brains. Briefly, the stripped rat brains were ground with liquid nitrogen in a Waring blender and then homogenized in 50 mM HEPES, 2 mM EGTA, 0.3 M sucrose, pH 7.4, with 10 strokes in a glass-Teflon homogenizer. The homogenate was spun at 100,000 × *g* for 28 min to pellet cell debris. The supernatant containing SVs was removed for further purification and the pellet was discarded. The supernatant was then layered onto a 1.5/0.6 M sucrose step gradient and spun at 260,000 × *g* for 72 min, after which SVs were removed from the interface between the sucrose layers. Vesicles were flash-frozen in separate 0.5 mL aliquots and stored at –80°C until needed.

SV labeling

Before labeling, the vesicles were dialyzed in a 10,000 MWCO Slide-a-Lyzer cassette (Pierce, Rockford, Illinois) against assay buffer (10 mM HEPES, 4 mM KCl, 4 mM $MgSO_4$, 0.3 M sucrose, pH 7.4) overnight at 4°C. After dialysis, the SVs were incubated with an excess of primary antibody against SV2A (polyclonal) or against synaptotagmin (monoclonal) at 20°C for 15 min. Next, the vesicles were incubated with a fluorescent secondary antibody (either Alexa Fluor 633 goat anti-rabbit IgG or Alexa Fluor 488 goat anti-rabbit IgG; Invitrogen, Carlsbad, CA) at 20°C for 15 min. Removal of excess antibody was accomplished by incubation with IgG-conjugated agarose beads specific for the primary antibody (rabbit IgG agarose; Sigma-Aldrich, St. Louis, MO) and the secondary antibody (anti-goat IgG agarose; Sigma-Aldrich) in two separate steps. Vesicles were incubated for 45 min at 20°C with each type of IgG-conjugated agarose bead, and the beads were then removed by centrifugation at 1000 × *g* for 2 min. The vesicles were stored on ice in assay buffer until just before the loading was performed. The same procedure was followed for GFP-transfected vesicles.

Fluorescence correlation spectroscopy measurements

For fluorescence correlation spectroscopy (FCS) measurements, fluorescently tagged SVs in solution (~30–50 μL) were placed on a glass coverslip above the objective. To ensure consistency in the measurements, we focused the laser probe volume at 25 μm above the surface of the coverslip into the sample droplet. The samples were excited with light from a 632.8 nm HeNe

Submitted June 2, 2009, and accepted for publication August 18, 2009.

*Correspondence: Chiu@chem.washington.edu

Editor: Petra Schwille.

0006-3495/09/11/2577/8 $2.00

doi: 10.1016/j.bpj.2009.08.032

laser (Coherent, Santa Clara, CA) and/or 488 nm light from a solid-state diode pumped laser (Sapphire; Coherent). Fluorescence was collected via an avalanche photodiode (APD SPCM-AQR-16; PerkinElmer, Fremont, CA). To initiate glutamate uptake, we added ATP and glutamate at the desired concentration to the SVs and allowed them to incubate at room temperature for 10 min. At the start of each experiment, calibration measurements were performed using 60 nm polystyrene beads. To produce the autocorrelation curve, sample fluorescence was collected for 2 min, with five autocorrelation curves collected for each sample droplet. Multiple data sets (3–6) were collected for each sample per day. The collected autocorrelation data were fitted to obtain the average diffusion coefficient of the particles. The standard deviations (SDs) of the percent change in average SV diameter were on the order of 5%.

FCS simulations

Details of the FCS simulation can be found in one of our previous publications (6). For this work, we investigated the effect of a heterogeneous sample on the FCS signal and the apparent diffusion coefficient obtained from that signal. Briefly, the simulation sample consisted of 40 spheres confined to a spherical volume, which was 8 μm in diameter. Each simulation represented an FCS measurement of 60 s. The nonglutamate vesicles were represented by spheres with a diameter of 60 nm. The loaded glutamate vesicles were represented by spheres with a range of diameters (66.5, 74.1, 83.0, 93.7, and 107.0 nm). For each loaded glutamate vesicles of given diameter, we ran a series of simulations with different percentages of loaded glutamate vesicles; the results were the average best-fit hydrodynamic diameters from 18 FCS simulations. Other details of the simulation, as well as the fitting procedure used to extract the diffusion coefficients from which the hydrodynamic diameters were obtained, were the same as those reported in Kuyper et al. (6).

Cryogenic electron microscopy

Cryogenic electron microscopy (cryo-EM) was performed on purified vesicles that were dialyzed into 230 mM glycine, 10 mM HEPES, 4 mM KCl, and 4 mM $MgSO_4$. For loaded vesicles, 1 mM glutamate and 1 mM ATP were added and allowed to equilibrate for 10 min at room temperature before freezing. Unloaded vesicles were used without further modification after the dialysis. The vesicles were applied to a holey carbon-coated grid, rapidly frozen in liquid ethane, and maintained at ~100 K with a Gatan (Pleasanton, CA) 626 cryoholder. Images were recorded on a Gatan 1024 × 1024 CCD camera mounted in a FEI Tecnai F30 electron microscope (FEI, Hillsboro, OR), which was operated at 300 kV at a nominal magnification of 49,000× and underfocused 10–20 μm. Two separate experiments were performed with the data from the two experiments collated into one set for presentation purposes. From these images, vesicle diameters were measured from the outer edge of the black ring, where two diameters orthogonal to one another were measured and averaged. There were a small number of membrane organelles with diameters > 100 nm in the images, which we excluded from the data set.

RESULTS

Measurements of SVs by FCS

We purified SVs from rat or mouse brains. For FCS experiments, the SVs were labeled with antibodies directed against SV-specific proteins (SV2A or synaptotagmin), which were in turn labeled with fluorescent secondary antibodies. FCS, a technique that measures the size of objects by measuring their diffusion, was performed on an in-house-built instrument (Fig. 1 *A*) (6,7). Fig. 1, *B* and *C*, show the raw time trace and the resultant autocorrelation curve, respectively, as SVs in solution transit the FCS probe volume. The FCS setup was calibrated with a range of size standards (20–200 nm fluorescent beads; Fig. 1 *D*), and our FCS measurements were checked for accuracy with 60 nm beads before each run. To label vesicles, we used an antibody against the membrane protein SV2A. SV2A is present on all glutamatergic vesicles in the central nervous system. Although its molecular action is not known, analyses of SV2A knockout mice indicate that it is not involved in neurotransmitter loading (8,9). The diffusion coefficient or hydrodynamic diameter for SV2A antibody-labeled SVs was measured with both single- and dual-color FCS. Up to five correlation curves were collected for each sample (unloaded, loaded, etc.) at one time, and each experiment was performed multiple times to confirm the results. The percent change was calculated for each day's collected data along with the relative SD of the percent change. The percent change from multiple days was collated to form a single data set from which the error bars are derived. It is important to note that each collection of correlation curves is a separate experiment; we are not attempting to distinguish between

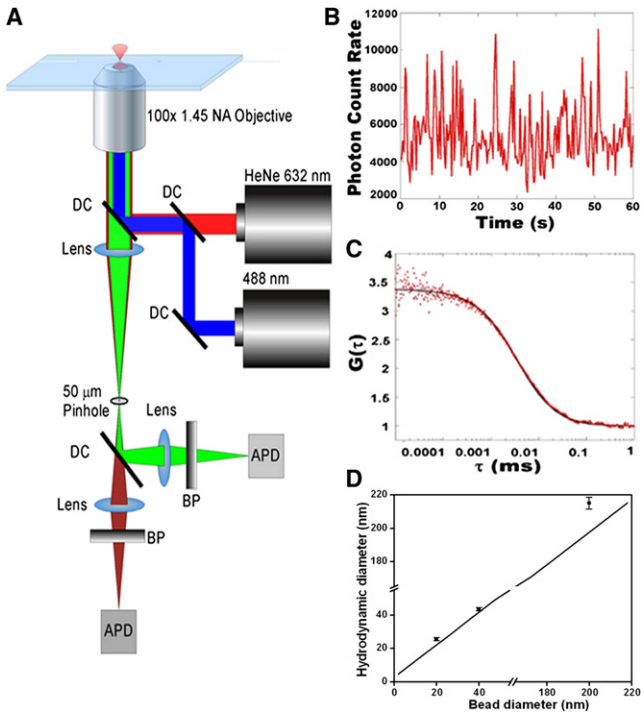

FIGURE 1 FCS setup and method. (*A*) Schematic of the in-house built instrument used to perform FCS. DC: dichroic mirror; APD: avalanche photodiode; BP: bandpass filter. (*B*) Typical raw time trace of the fluorescence signals obtained from antibody-labeled SVs and (*C*) the corresponding autocorrelation function. (*D*) Calibration plot for our FCS instrument using fluorescent beads of known diameters (24 ± 4 nm, 36 ± 5 nm, 60 ± 3 nm, and 210 ± 10 nm, ± SD). The hydrodynamic diameters of four different-sized polystyrene beads were measured to ensure that the FCS setup was calibrated for a wide range of sizes. The linear correlation coefficient is 0.99.

unloaded and loaded vesicles that are present in the same solution with FCS.

To determine whether the presence of antibodies affected the diffusion coefficient of the SVs, we measured SVs in the presence or absence of antibodies. These studies were performed using vesicles isolated from mice expressing synaptopHluorin (10). SynaptopHluorin vesicles have a pH-sensitive GFP fused to the lumenal domain of the vesicle protein VAMP/synaptobrevin. This provides a fluorescent vesicle whose diffusion coefficient can be measured by FCS in the absence of antibodies. We did not perform loading experiments with synaptopHluorin vesicles because the pH-sensitive GFP is not fluorescent at pH < 6.0. As SVs load glutamate, the interior of the vesicle acidifies to a pH of ~5.5, and thus the synaptopHluorin vesicles become invisible when they load glutamate. We measured the diffusion coefficient of synaptopHluorin vesicles and antibody-labeled (anti-synatpotagmin primary antibody and Alexa633 secondary antibody) synaptopHluorin vesicles. The diffusion coefficients were identical within the error of the assay, which shows that the measured diffusion coefficient is not affected by the presence of a few antibodies on the vesicle exterior (see Fig. S1 and Table S1 in the Supporting Material).

Isolated SVs double their volume upon loading with glutamate

SVs purified from brain do not contain glutamate, due to transmitter leakage during purification in the absence of ATP (11). Incubating SVs in a loading buffer (LB) containing ATP and glutamate induces refilling (12,13) of vesicles. We compared the hydrodynamic diameter of ''empty'' or ''unloaded'' SVs with that of vesicles filled with glutamate. We found that the filling of SVs caused the measured hydrodynamic diameter to increase by 23.9% $\pm$ 4.8% (SD of the percent change; Fig. 2 *A*). Removal of either glutamate or ATP prevented this observed size increase (Fig. 2 *A*).

The dramatic increase in SV size did not occur when the uptake of glutamate was blocked by competitive (Trypan blue) (14) or noncompetitive (rose Bengal) (15) inhibitors of the vesicular glutamate transporter, VGLUT1 (Fig. 2 *A*). The size increase was also blocked when the electrochemical gradient required for uptake was abolished, as in the absence of ATP or in the presence of bafilomycin, an inhibitor of the H^+/ATPase (16) (Fig. 2, *A* and *B*). These results show that the size increase is a direct consequence of glutamate loading.

We found that the increase in vesicle size depended on the extravesicular glutamate concentration up to 0.25 mM (Fig. 2 *B*), consistent with the observation that VGLUT1 activity is modulated by external glutamate concentrations (17). Additionally, the observed size increase also depended on the extravesicular concentration of ATP (Fig. 2 *C*). Below ~0.8 mM ATP, we did not observe any appreciable size increase, which is consistent with the previously measured apparent K_m (0.8–2 mM) for exogenous ATP determined under standard assay conditions for glutamate loading (18). Therefore, the observed increase in vesicle size again appears to be a direct result of the loading of neurotransmitters into the vesicle.

For our FCS measurements, we failed to observe any size increase when VGLUT1 was labeled directly with antibodies (data not shown), likely because direct attachment of antibodies to VGLUT1 interfered with the proper functioning of the transporter. Therefore, we used antibodies against a protein present on all SVs (SV2A or synaptotagmin) (19). As a result, the actual size increase for glutamatergic vesicles is likely higher because a fraction of the vesicles in our preparation are not glutamatergic. To understand how the presence of unloaded vesicles might affect average FCS values, we carried out a series of simulations in which we calculated the size increase of loaded glutamatergic vesicles as a percentage of the measured FCS diameter for unloaded vesicles and the percentage of glutamatergic vesicles present (Fig. 2 *D*). We estimate that glutamatergic vesicles constitute ~80% of all SVs, based on the observation that GABAergic vesicles make up ~16% of the total vesicle population (20), and an estimate that cholinergic and aminergic vesicles are present at ~4%. Therefore, if we estimate that ~20% of the vesicles are unloaded and do not change size, the actual hydrodynamic diameter increase is 31.7% (Fig. 2 *D*, *inset*).

To rule out vesicle aggregation or fusion as a cause of the observed size increase, we measured average fluorescence intensity of unloaded and loaded vesicles as they transited the FCS probe volume (Fig. 3 *A*). We found the average intensity to be identical for unloaded and loaded vesicles (Fig. 3 *A*), indicating that the observed size increase was not caused by the aggregation or fusion of two or more vesicles. Aggregation or fusion of vesicles should produce an increase in the average intensity because more fluorescent antibodies would be bound to the larger vesicle. To further dismiss fusion as a cause, we measured vesicle size in the presence of the calcium chelator EGTA, which inhibits Ca^{2+}-induced vesicle fusion. Fig. 3 *B* shows that SVs treated with EGTA exhibited the same size increase as untreated SVs; therefore, Ca^{2+}-induced fusion is not responsible for the size increase.

We also checked to see whether a difference in osmotic pressure would cause the vesicles to change size. For this experiment, SVs in buffer (10 mM HEPES, 4 mM KCl, 4 mM $MgSO_4$, 320 mM sucrose, pH 7.4) were diluted with distilled water by 50% and then allowed to sit for 10 min at room temperature. We found that the measured hydrodynamic size of these vesicles was no different from that of unloaded vesicles in buffer. The pressure difference created by changing the osmotic strength of the buffer by half does not by itself appear to be sufficient to cause the vesicles to change size appreciably.

Most importantly, we were able to reverse the size increase by treating loaded SVs with exogenous ATPase (Fig. 3 *B*), which led to a rundown of the electrochemical gradient and

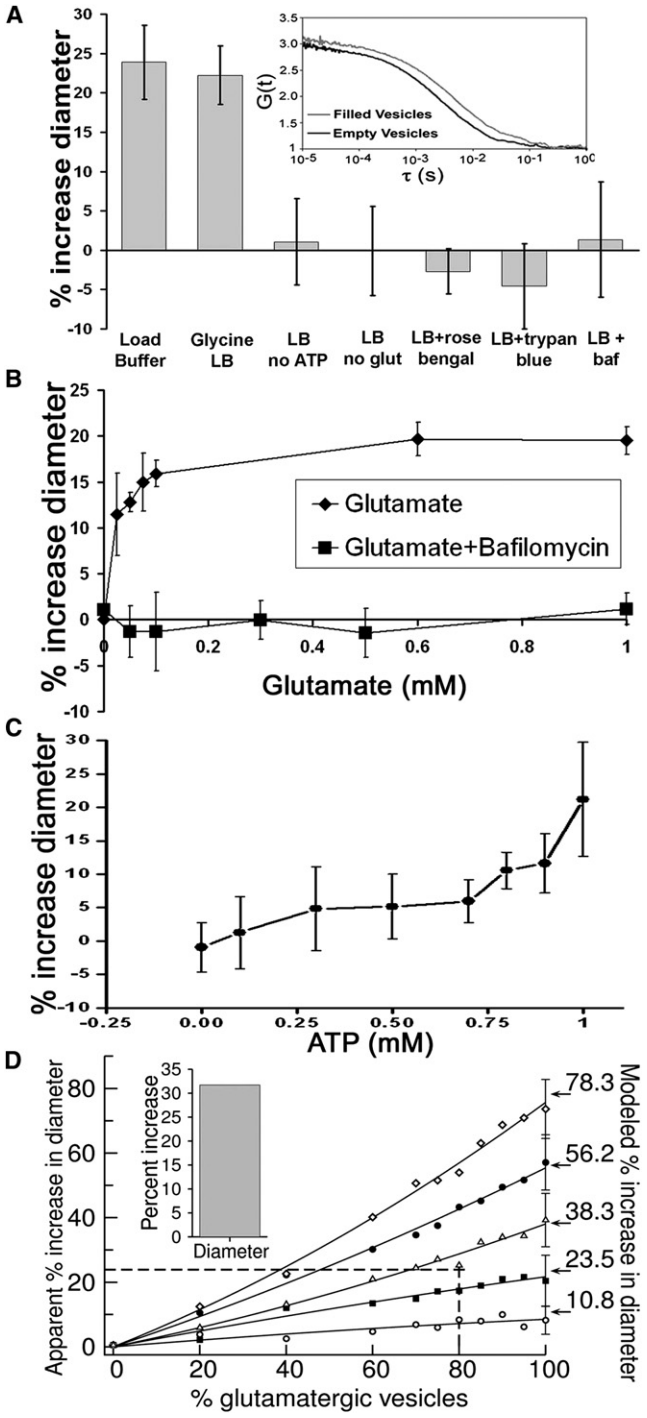

FIGURE 2 SVs show an increase in size upon loading with glutamate. All plots show percent change ± SD of percent change. (*A*) Plot showing the change in hydrodynamic diameter of rat SVs under various loading conditions. The LB consisted of 10 mM HEPES, 4 mM KCl, 4 mM $MgSO_4$, 320 mM sucrose, 1 mM ATP, and 1 mM glutamate at pH 7.4; ATP and glutamate were added separately and the vesicles were allowed to load for 10 min at room temperature. The glycine LB (buffer used in cryo-EM) consisted of 10 mM HEPES, 4 mM KCl, 4 mM MgSO4, 230 mM glycine, 1 mM ATP, and 1 mM glutamate at pH 7.4. "LB no ATP": LB without ATP; "LB no glut": LB without glutamate; "LB + rose Bengal": LB with 1 μM rose Bengal; "LB + trypan blue": LB with 1.25 μM Trypan blue; "LB + baf": LB with 0.6 mM bafilomycin. Inset shows the visible difference in the autocorrelation function between "unloaded" vesicles and "loaded" vesicles. (*B*) Graph showing percent increase in hydrodynamic diameter of loaded SVs as a function of the extravesicular glutamate concentration; ATP concentration was 1 mM for all, and bafilomycin concentration was 0.6 mM for the lower curve. (*C*) Graph showing the percent increase in hydrodynamic diameter of loaded vesicles as a function of extravesicular ATP concentration; glutamate concentration was 1 mM for all. (*D*) Simulation showing the apparent increase in hydrodynamic diameter versus percentage of glutamate vesicles in our FCS samples. The simulated unloaded and nonglutamatergic vesicles in the sample have a hydrodynamic diameter of 60 nm, whereas the loaded glutamate vesicles were simulated with hydrodynamic diameters of (○) 66.5, (■) 74.1, (Δ) 83.0, (●) 93.7, and (◇) 107.0 nm. Each point for 60–100% glutamatergic vesicles is the average of best-fit results for 18 simulations. The results for the 20% and 40% points are the average from six simulations. The result for the 0% point is the average from 12 simulations. The diameters have all been converted to percent increases (shown on the right of the plot) for comparison with our experimental measurements. Typical values of the SD of the best fit results are shown for some of the points, and solid lines have been drawn to guide the eye. The horizontal dashed line was drawn at 23.9% increase, the measured percent increase in the hydrodynamic diameter of the loaded SVs measured by FCS. The vertical dashed line is drawn at 80%, which is the estimate of the percentage of glutamatergic vesicles. The intersection of the two dashed lines is used to estimate the percentage increase of the hydrodynamic diameter of the glutamatergic vesicles only.

leakage of glutamate. SVs were loaded with glutamate and ATP at room temperature, and then treated with 0.6 U ATPase for 2 min. The correlation curves revealed that the SVs had returned to the unloaded size, indicating that the size increase is reversible. Whatever changes the vesicles undergo during loading, the process is reversible once the loading conditions are removed. It is difficult to imagine a fusion event that could be reversed due to the presence of ATPase. These data also suggest an internal control for the FCS measurements, as any unforeseen environmental differences between unloaded and loaded vesicle solutions would not be reversed by the addition of ATPase. Therefore, the measured size increase appears to be due to the vesicle filling with transmitter and is not an artifact of the experimental design.

Cryo-EM

To determine whether the increase in hydrodynamic diameter represents an actual expansion of the vesicle, we conducted cryo-EM studies on unstained, plunge-frozen vesicles imaged directly in vitrified ice (Fig. 4). Cryo-EM images were taken of unloaded SVs ($n = 200$) and SVs incubated under loading conditions ($n = 186$), and analyzed. Fig. 4 *A* shows a histogram distribution of the diameters of unloaded and loaded vesicles, demonstrating a shift to larger size upon filling. To quantify the size increase, we graphed the data as a cumulative probability plot (Fig. 4 *B*). From this plot, we calculate that the average vesicle diameter (mean ± SD) increased from 45.7 ± 13.9 nm to 56.9 ± 17.1 nm, corresponding to a 24.5% ± 1.2% increase in diameter and 91.8% ± 4.6% increase in volume (Fig. 4 *A*, *inset*). To correct for the presence of nonglutamatergic vesicles, we

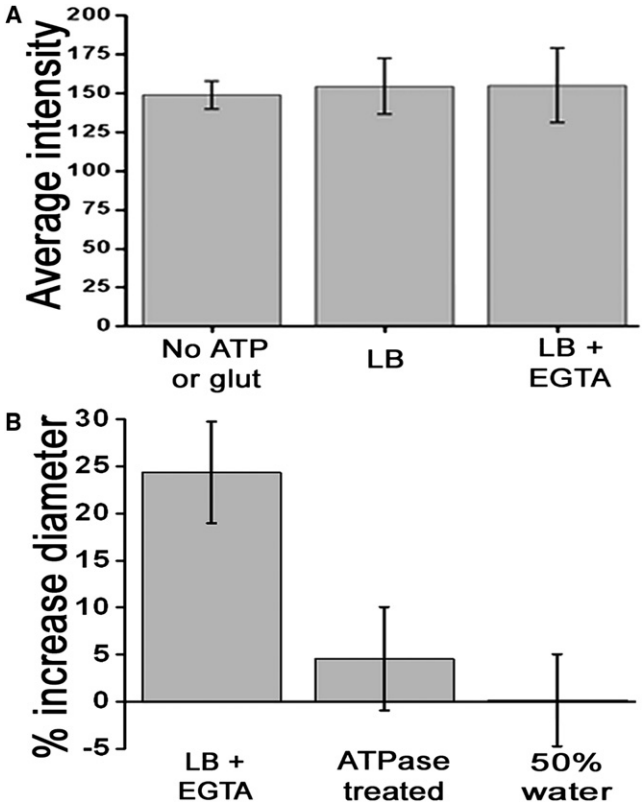

FIGURE 3 SVs are not aggregated or fused under our measurement conditions. (*A*) A plot of the average fluorescence intensity (arbitrary units) ± SD of SVs as they transit the laser probe volume under the three conditions indicated on the *x* axis. All measurements were performed in LB consisting of 10 mM HEPES, 4 mM KCl, 4 mM $MgSO_4$, 320 mM sucrose, 1 mM ATP, and 1 mM glutamate at pH 7.4, except for ''Unloaded'' vesicles, which were in LB without glutamate and ATP, and ''Loaded w/ EGTA'' vesicles, which were in LB plus 1 mM EGTA. (*B*) Vesicles loaded under the following conditions: 1, LB plus 1 mM EGTA (''EGTA''); 2, loaded in LB and then treated with 0.6U ATPase (''ATPase'') for 2 min; and 3, unloaded vesicles diluted 50% by the addition of distilled water (''50% Water''). The plot gives the percent change ± SD of percent change. For all experiments, loading was performed at room temperature for 10 min.

subtracted 20% of the unloaded vesicle (*shaded bars*) population in each size bin from the number of loaded vesicles (*hatched bars*). This yielded an average diameter for the loaded vesicles of 59.1 ± 5.6 nm, which corresponds to an increase in diameter of 29.3% (Fig. 4 *C*). The increase in vesicle size, therefore, appears to be the result of an expansion of the vesicle.

Vesicles lacking SV2A do not show a size increase with loading

We found that the size increase required the presence of SV2A (Fig. 5). SVs isolated from either SV2A knockout (AKO) or SV2A/SV2B double knockout (DKO) mice (labeled with anti-synaptotagmin) did not exhibit a size increase upon loading with glutamate, whereas SVs from wild-type (WT) mice did. In WT vesicles (labeled with anti-synaptotagmin), the size increase upon loading was similar to that measured with SVs from rat (20.8% ± 1.8%; Fig. 5 *A*). SVs from mice heterozygous (Het) for the SV2A gene were also tested. Het SV2A vesicles, which have roughly half the amount of SV2A as homozygous vesicles (Fig. 5 *B*), showed a reduced size increase of 15.2% ± 3.9% upon loading with glutamate. Thus, the change in vesicle size involves more proteins than just the proteins involved in neurotransmitter loading (i.e., VGLUT or V_0-ATPase).

DISCUSSION

In contrast to previous in vivo observations (3,4), our in vitro measurements of isolated SVs in solution indicate that SVs can undergo large size changes without sources of additional lipids or proteins, and that this ability to change size requires the presence of SV2A. Change in the vesicle structure could be induced by the establishment of an electrochemical gradient leading to the presence of luminal glutamate, which could influence the conformation of vesicle membrane proteins.

The size change of glutamatergic vesicles we report here is strikingly similar to irreversible and reversible size changes observed in viruses. During maturation or cell entry, viral capsids can undergo irreversible expansion (for phages, typically a ~20% increase in diameter, leading to a near doubling of volume) or contraction (HIV and other lentiviruses, papillomaviruses, and an insect virus, *Nudaurelia capensis* ω-virus) (21). These significant dimensional changes, which are critical for viral function, are brought about by substantial alterations of the associated capsid proteins. Reversible size changes also occur in virus capsids. In the case of the *Nudaurelia capensis* ω-virus capsid, a normally irreversible shrinkage is rendered reversible via changes in pH in the absence of a required proteolytic cleavage (22). Cowpea chlorotic mottle virus (CCMV) reversibly expands and contracts with changes in pH and Mg^{2+} or Ca^{2+} concentration (23). Poliovirus (24) and Flock House virus (25) undergo a reversible ''breathing'' transition that exposes internal protein entities to antibodies and proteases. This transition likely produces a larger particle as an intermediate in the transition, a final product, or both. In similarity to reversible viral transitions, SVs are apparently able to undergo large structural changes as a function of glutamate loading.

Fig. 6 provides an island model for the SV, which shows a size increase similar to that experienced by CCMV, and an internal-matrix swelling model. In Fig. 6 *A*, SVs are modeled as having white ''islands'' of nonexpandable components composed mostly of lipid molecules. The ''islands'' are surrounded by a gray ''sea'' comprised of expandable components, most likely protein clusters (26). As the SV loads glutamate, the proteins undergo a conformational change, leading to an expansion of the ''sea''. This model mimics the reversible expansion of the CCMV (Fig. 6 *B*), which increases 20% in diameter. CCMV expands via the intercapsomere connections, with the capsomere cores remaining the

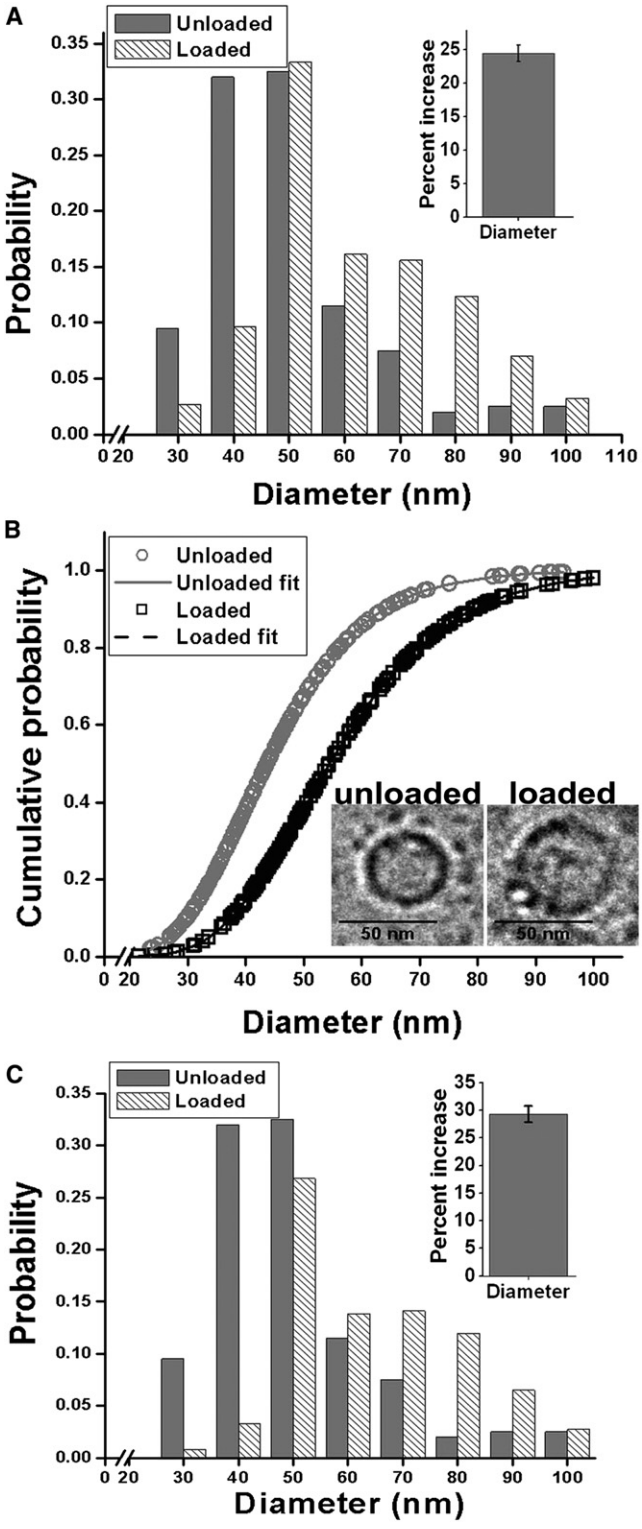

FIGURE 4 Cryo-EM measurements of vesicle diameter reveal an increase in size upon glutamate loading. (*A*) Histogram showing the distribution of diameters for unloaded and loaded SVs in glycine LB (10 mM HEPES, 4 mM KCl, 4 mM $MgSO_4$, 230 mM glycine, 1 mM ATP, and 1 mM glutamate at pH 7.4). Inset shows percent increase in diameter for loaded vesicles. (*B*) Cumulative probability plot of diameters for unloaded and loaded vesicles. Plots were fit with a lognormal distribution to obtain a diameter of 45.7 ± 13.9 nm (mean ± SD) for unloaded and 56.9 ± 17.1 nm for loaded vesicles. Inset shows representative pictures for unloaded and loaded vesicles. (*C*) Histogram showing the distribution in diameters for glutamatergic vesicles only, which was calculated by subtracting from each size bin 20% of the number of empty vesicles (*shaded bars*) from the number of loaded vesicles (*hatched bars*); inset shows this corrected percent increase in diameter for loaded glutamatergic vesicles.

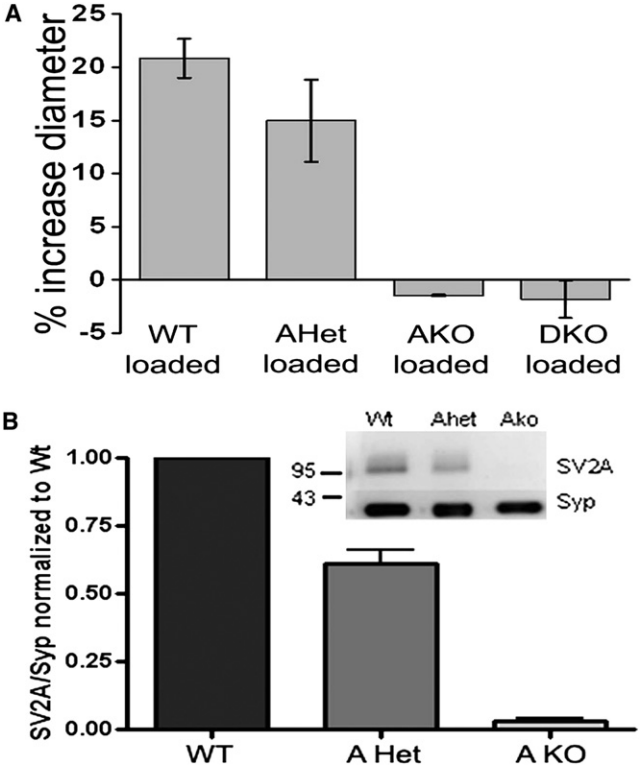

FIGURE 5 Dependence of vesicle size increase on the presence of SV2A. (*A*) A bar plot showing the increase in vesicle size requires SV2A. SVs isolated from WT mice, heterozygous SV2A mice (AHet), SV2A knockout mice (AKO), or SV2A/SV2B double knockout mice (DKO) were loaded at room temperature for 10 min in LB (10 mM HEPES, 4 mM KCl, 4 mM $MgSO_4$, 320 mM sucrose, 1 mM ATP, and 1 mM glutamate at pH 7.4). These vesicles were all labeled with antibodies against synaptotagmin. (*B*) Western blot comparing SV2A and synaptophysin content in WT mice, AHet mice, and AKO mice. The bar graph shows the ratio of SV2A expression versus the expression of synaptophysin, a common SV marker protein, normalized to the expression level in WT mice. Proteins were probed with a polyclonal antibody directed against SV2A and a polyclonal antibody directed against synaptophysin. As anticipated, AHet vesicles ($n = 4$) have about half the amount of expressed SV2A as WT vesicles ($n = 4$), whereas vesicles from AKO ($n = 3$) mice contain no SV2A. All vesicles exhibited similar levels of synaptophysin.

same size. The intercapsomere connections are comprised of protein domains, analogously to the SV protein clusters that have been reported upon detergent solubilization (26).

Since vesicles without SV2A did not increase in size, but still accumulate glutamate in vivo (8), SV2A likely contributes to the structural change that vesicles undergo as a consequence of glutamate loading. SV2A is predicted to contain 12 transmembrane domains, making it one of the larger SV proteins. A recent tomography study of SV2A suggests

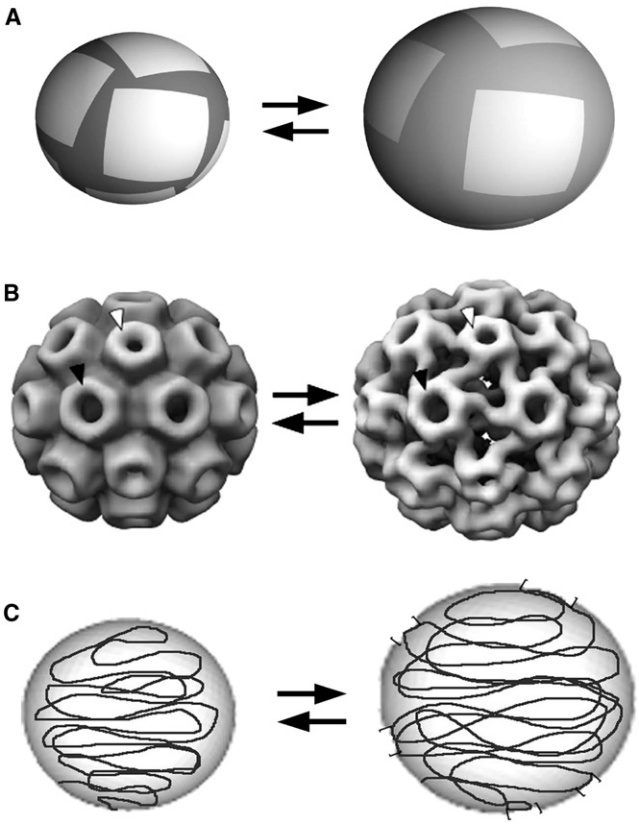

FIGURE 6 Models of SV expansion. (*A*) Island model. In this model (*left*), nonexpandable components (most likely lipids) are modeled as white islands corresponding to ~65% of the surface area. The remaining surface area (*gray*) represents expandable components, most likely proteins. Loading glutamate causes the protein "sea" to expand, whereas the "islands" do not change size appreciably. Holes may form in the islands or the sea, but can be plugged by expansion of the internal matrix. The expanded model (*right*) represents a ~25% increase in diameter. The size, shape, and arrangement of islands in these depictions are arbitrary. (*B*) Our model is analogous to the reversible expansion of CCMV. Three-dimensional reconstructions of the unexpanded (*left*) and expanded (*right*) states are shown (23). Unexpanded CCMV is ~29 nm in diameter and is formed by pentameric (*white arrowhead*) and hexameric (*black arrowhead*) oligomers known as capsomeres. The expanded form is ~20% larger in diameter. SVs could expand in a similar manner. Analogously to the "islands" in our model, the cores of CCMV hexamers and pentamers remain the same size, whereas the intercapsomere connections expand. In CCMV, the expandable intercapsomere connections are protein domains. (*C*) Matrix-swelling model. In this model, the vesicle size increase is caused by expansion of the internal matrix upon glutamate loading. The internal matrix expands and pushes the membrane outward, possibly causing the formation of holes in the membrane (shown as brackets in the membrane). Loaded glutamate is held in the internal matrix, thus keeping the vesicle from leaking glutamate after the expansion occurs.

that it exists in two conformations: a cytoplasmic-facing conformation and an intravesicular-facing conformation (27). These conformational differences suggest a high degree of flexibility in the SV2A structure. Additionally, SV2A is a distant relative of prestin, a novel motor protein that has been proposed to produce changes in hair cell length in the auditory system (28,29). Like SV2A, prestin shares structural features with solute transporters, though it does not appear to act as a transporter. In response to changes in membrane potential, prestin undergoes a large conformational change that can change cell shape by as much as 5% (29). We note, however, that these predicted changes in SV2 conformation are not of sufficient magnitude to completely account for the size changes reported here.

In cholinergic vesicles, SV2A is a keratin sulfate proteoglycan (30), and its large sugar moieties appear to constitute a significant proportion of the glycolytic matrix in SVs (31). Similar matrices have been shown to expand in size, doubling their volume, with changes in ionic strength (31). This suggests that the vesicular matrix may undergo a structural transition due to the formation of the electrochemical gradient or the presence of neurotransmitter inside the vesicle. The existence of an insoluble polymer-like matrix would ensure that vesicular contents are retained if holes form in the vesicle membrane as a result of the size increase (32). Fig. 6 *C* depicts this scenario as an internal-matrix swelling model. In this model, neurotransmitter is concentrated within an internal matrix that needs to undergo swelling before transmitter can be released (33). SV2A modulates the number of vesicles competent for fusion (8,34,35). Combining the fact that the loss of SV2A reduces release probability with the finding that in the absence of SV2A the vesicles do not increase in size upon glutamate loading, a model emerges in which swelling of the SV2-linked internal matrix may signal that vesicles are ready for release.

Alternatively, it is possible that, rather than playing a direct role in the size change, SV2A plays an indirect role by influencing the protein composition of vesicles. Loss of SV2 has been linked to changes in the levels of other SV proteins (36); thus, vesicles lacking SV2A, which is the major isoform of SV2 in vertebrate CNS, may lack a protein component required for the size change seen in WT vesicles. SV2A may contribute to changes in vesicle size in multiple ways. Future research will determine whether the size change reported here is a direct or indirect action of SV2A, and how this size change contributes to vesicle functioning.

SUPPORTING MATERIAL

A figure, a table, and a reference are available at http://www.biophysj.org/biophysj/supplemental/S0006-3495(09)01393-9.

We thank G. Milne for help with image processing.

K.L.B. was supported by the National Science Foundation through a Graduate Student Fellowship. D.T.C. acknowledges a fellowship from the Sloan Foundation. This work was supported by the National Institutes of Heath (NS 052637 and NS 062725), the Keck Foundation, and the National Science Foundation (NSF CHE 0342956), and by institutional support to D.M.B.

REFERENCES

1. Takamori, S., M. Holt, K. Stenius, E. A. Lemke, M. Gronborg, et al. 2006. Molecular anatomy of a trafficking organelle. *Cell.* 127:831–846.

2. Sudhof, T. C. 2004. The synaptic vesicle cycle. *Annu. Rev. Neurosci.* 27:509–547.

3. Daniels, R. W., C. A. Collins, K. Chen, M. V. Gelfand, D. E. Featherstone, et al. 2006. A single vesicular glutamate transporter is sufficient to fill a synaptic vesicle. *Neuron.* 49:11–16.

4. Colliver, T. L., S. J. Pyott, M. Achalabun, and A. G. Ewing. 2000. VMAT-mediated changes in quantal size and vesicular volume. *J. Neurosci.* 20:5276–5282.

5. Needham, D., and R. S. Nunn. 1990. Elastic deformation and failure of lipid bilayer membranes containing cholesterol. *Biophys. J.* 58: 997–1009.

6. Kuyper, C. L., B. S. Fujimoto, Y. Zhao, P. G. Schiro, and D. T. Chiu. 2006. Accurate sizing of nanoparticles using confocal correlation spectroscopy. *J. Phys. Chem. B.* 110:24433–24441.

7. Elson, E. L., and D. Magde. 1974. Fluorescence correlation spectroscopy. I. Conceptual basis and theory. *Biopolymers.* 13:1–27.

8. Custer, K. L., N. S. Austin, J. M. Sullivan, and S. M. Bajjalieh. 2006. Synaptic vesicle protein 2 enhances release probability at quiescent synapses. *J. Neurosci.* 26:1303–1313.

9. Crowder, K. M., J. M. Gunther, T. A. Jones, B. D. Hale, H. Z. Zhang, et al. 1999. Abnormal neurotransmission in mice lacking synaptic vesicle protein 2A (SV2A). *Proc. Natl. Acad. Sci. USA.* 96:15268–15273.

10. Li, Z., J. Burrone, W. J. Tyler, K. N. Hartman, D. F. Albeanu, et al. 2005. Synaptic vesicle recycling studied in transgenic mice expressing synaptopHluorin. *Proc. Natl. Acad. Sci. USA.* 102:6131–6136.

11. Carlson, M. D., and T. Ueda. 1990. Accumulated glutamate levels in the synaptic vesicle are not maintained in the absence of active transport. *Neurosci. Lett.* 110:325–330.

12. Thompson, C. M., E. Davis, C. N. Carrigan, H. D. Cox, R. J. Bridges, et al. 2005. Inhibitor of the glutamate vesicular transporter (VGLUT). *Curr. Med. Chem.* 12:2041–2056.

13. Ozkan, E. D., and T. Ueda. 1998. Glutamate transport and storage in synaptic vesicles. *Jpn. J. Pharmacol.* 77:1–10.

14. Roseth, S., E. M. Fykse, and F. Fonnum. 1998. Uptake of L-glutamate into synaptic vesicles: competitive inhibition by dyes with biphenyl and amino- and sulphonic acid-substituted naphthyl groups. *Biochem. Pharmacol.* 56:1243–1249.

15. Ogita, K., K. Hirata, D. G. Bole, S. Yoshida, Y. Tamura, et al. 2001. Inhibition of vesicular glutamate storage and exocytotic release by rose Bengal. *J. Neurochem.* 77:34–42.

16. Drose, S., and K. Altendorf. 1997. Bafilomycins and concanamycins as inhibitors of V-ATPases and P-ATPases. *J. Exp. Biol.* 200:1–8.

17. Wilson, N. R., J. Kang, E. V. Hueske, T. Leung, H. Varoqui, et al. 2005. Presynaptic regulation of quantal size by the vesicular glutamate transporter VGLUT1. *J. Neurosci.* 25:6221–6234.

18. Naito, S., and T. Ueda. 1985. Characterization of glutamate uptake into synaptic vesicles. *J. Neurochem.* 44:99–109.

19. Bajjalieh, S. M., G. D. Frantz, J. M. Weimann, S. K. McConnell, and R. H. Scheller. 1994. Differential expression of synaptic vesicle protein 2 (SV2) isoforms. *J. Neurosci.* 14:5223–5235.

20. Takamori, S., D. Riedel, and R. Jahn. 2000. Immunoisolation of GABA-specific synaptic vesicles defines a functionally distinct subset of synaptic vesicles. *J. Neurosci.* 20:4904–4911.

21. Steven, A. C., J. B. Heymann, N. Cheng, B. L. Trus, and J. F. Conway. 2005. Virus maturation: dynamics and mechanism of a stabilizing structural transition that leads to infectivity. *Curr. Opin. Struct. Biol.* 15:227–236.

22. Taylor, D. J., N. K. Krishna, M. A. Canady, A. Schneemann, and J. E. Johnson. 2002. Large-scale, pH-dependent, quaternary structure changes in an RNA virus capsid are reversible in the absence of subunit autoproteolysis. *J. Virol.* 76:9972–9980.

23. Speir, J. A., S. Munshi, G. Wang, T. S. Baker, and J. E. Johnson. 1995. Structures of the native and swollen forms of cowpea chlorotic mottle virus determined by X-ray crystallography and cryo-electron microscopy. *Structure.* 3:63–78.

24. Li, Q., A. G. Yafal, Y. M. Lee, J. Hogle, and M. Chow. 1994. Poliovirus neutralization by antibodies to internal epitopes of VP4 and VP1 results from reversible exposure of these sequences at physiological temperature. *J. Virol.* 68:3965–3970.

25. Bothner, B., X. F. Dong, L. Bibbs, J. E. Johnson, and G. Siuzdak. 1998. Evidence of viral capsid dynamics using limited proteolysis and mass spectrometry. *J. Biol. Chem.* 273:673–676.

26. Bennett, M. K., N. Calakos, T. Kreiner, and R. H. Scheller. 1992. Synaptic vesicle membrane proteins interact to form a multimeric complex. *J. Cell Biol.* 116:761–775.

27. Lynch, B. A., A. Matagne, A. Brannstrom, A. von Euler, M. Jansson, et al. 2008. Visualization of SV2A conformations in situ by the use of protein tomography. *Biochem. Biophys. Res. Commun.* 375:491–495.

28. Zheng, J., W. Shen, D. Z. He, K. B. Long, L. D. Madison, et al. 2000. Prestin is the motor protein of cochlear outer hair cells. *Nature.* 405:149–155.

29. Dallos, P., and B. Fakler. 2002. Prestin, a new type of motor protein. *Nat. Rev. Mol. Cell Biol.* 3:104–111.

30. Wagner, J. A., S. S. Carlson, and R. B. Kelly. 1978. Chemical and physical characterization of cholinergic synaptic vesicles. *Biochemistry.* 17:1199–1206.

31. Reigada, D., I. Diez-Perez, P. Gorostiza, A. Verdaguer, I. Gomez de Aranda, et al. 2003. Control of neurotransmitter release by an internal gel matrix in synaptic vesicles. *Proc. Natl. Acad. Sci. USA.* 100:3485–3490.

32. Rahamimoff, R., and J. M. Fernandez. 1997. Pre- and postfusion regulation of transmitter release. *Neuron.* 18:17–27.

33. Vautrin, J. 2009. SV2 frustrating exocytosis at the semi-diffusor synapse. *Synapse.* 63:319–338.

34. Xu, T., and S. M. Bajjalieh. 2001. SV2 modulates the size of the readily releasable pool of secretory vesicles. *Nat. Cell Biol.* 3:691–698.

35. Chang, W. P., and T. C. Sudhof. 2009. SV2 renders primed synaptic vesicles competent for Ca^{2+} -induced exocytosis. *J. Neurosci.* 29:883–897.

36. Lazzell, D. R., R. Belizaire, P. Thakur, D. M. Sherry, and R. Janz. 2004. SV2B regulates synaptotagmin 1 by direct interaction. *J. Biol. Chem.* 279:52124–52131.